

# Activation of a Floral Homeotic Gene in *Arabidopsis*

Maximilian A. Busch,\* Kirsten Bomblies,\* Detlef Weigel†

The patterned expression of floral homeotic genes in *Arabidopsis* depends on the earlier action of meristem-identity genes such as *LEAFY*, which encodes a transcription factor that determines whether a meristem will generate flowers instead of leaves and shoots. The *LEAFY* protein, which is expressed throughout the flower, participates in the activation of homeotic genes, which are expressed in specific regions of the flower. Analysis of a *LEAFY*-responsive enhancer in the homeotic gene *AGAMOUS* indicates that direct interaction of *LEAFY* with this enhancer is required for its activity in plants. Thus, *LEAFY* is a direct upstream regulator of floral homeotic genes.

The appearance of individual *Arabidopsis* flowers is marked by the expression of several floral meristem-identity genes, including *LEAFY* (*LFY*), *APETALA1* (*API*), and *CAULIFLOWER*. Inactivation and overexpression of these genes cause opposite phenotypes, indicating that they act as developmental switches (1). A particularly dramatic loss-of-function phenotype is seen in *lfy* mutants, in which early arising flowers are replaced by leaves with associated shoots (2, 3). About 2 days after an individual flower has been initiated, three classes of homeotic genes, A, B, and C, are expressed in distinct, overlapping patterns within the developing flower. Both loss- and gain-of-function studies have shown that the patterned activities of ABC genes are responsible for the stereotypic sequence of sepals, petals, stamens, and carpels that form from the periphery to the center of the flower (4). In *Arabidopsis*, C function is specified by the MADS box gene *AGAMOUS* (*AG*), which confers stamen and carpel identity and which is normally expressed in the center of the flower (5, 6).

Although the function of *LFY* as a switch for floral identity indicates that *LFY* is formally an upstream regulator of *AG*, the effects of *lfy* mutations on *AG* expression are complex. Not all flowers of strong *lfy* mutants are replaced by leaves and shoots, and although *AG* RNA expression is delayed in the more flowerlike structures of *lfy* mutants, it eventually reaches levels that are similar to those in wild-type flowers (7). In addition, *AG* is ectopically expressed in later-developing flowers as well as in the stem of *lfy* mutants, indicating not only a positive but also a negative role of *LFY* in *AG* regulation. Similarly, the snapdragon *LFY* ortholog *FLORICAULA* (*FLO*) has both positive and

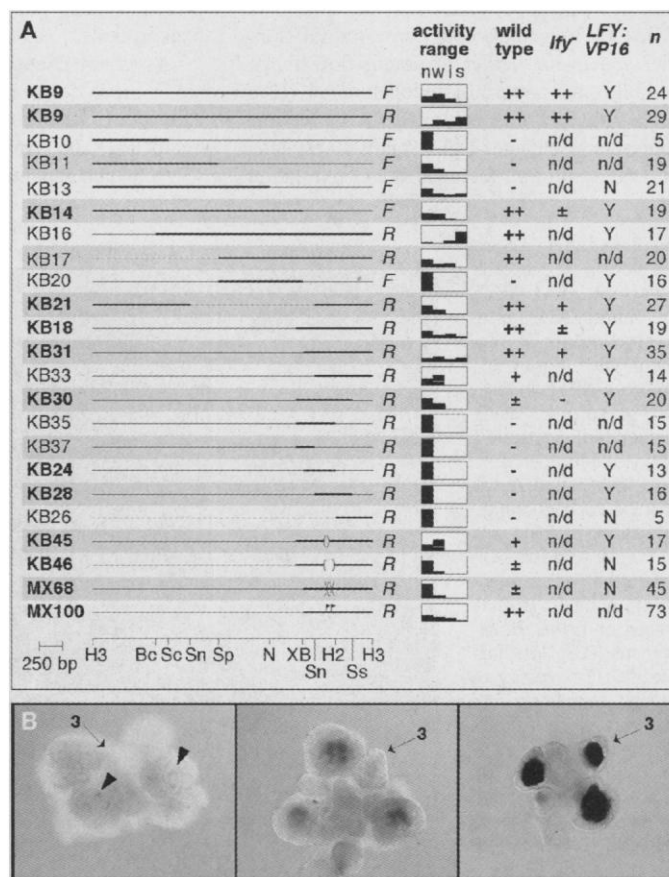
negative roles in the regulation of the *AG* ortholog *PLENA* (*PLE*) (8, 9). That *FLO* can activate *PLE* nonautonomously suggests that the effects of *FLO* and *LFY* on *PLE* and *AG* need not be direct (8).

Control of floral identity by *LFY* can be

genetically separated from a role of *LFY* in the later process of ABC gene regulation (10). Genetic arguments also suggested that the primary effect of *LFY* on *AG* is activation (10). In plants that expressed an activated form of *LFY* protein, *LFY:VP16*, *AG* RNA was detected earlier, ectopically, and at elevated levels when compared with wild-type flowers, suggesting that *LFY* normally interacts with region-specific coregulators that restrict *AG* expression to a subset of *LFY*-expressing cells (10).

To dissect the interaction between *LFY* and *AG*, we identified enhancers responsible for transcriptional activation of *AG* using transgenic plants that expressed the bacterial  $\beta$ -glucuronidase (*GUS*) gene under the control of various *AG* sequences. The second intron of *AG*, whose location largely coincides with a 3-kb *Hind* III restriction fragment, is required for *AG*-typical expression of a chimeric gene that encodes a translational fusion of *AG* to *GUS* (11). This *Hind* III fragment (12) contains transcriptional en-

**Fig. 1. AG enhancer dissection. (A)** Diagram of reporter constructs carrying *AG* genomic fragments in front of a minimal promoter driving *GUS* (19). Reporters discussed in the text or shown in Figs. 2 and 3 are in bold. MX68 carries the *AG* I m1 and *AG* II m1 mutations. MX100 carries *AG* I m2 and *AG* II m2 (Fig. 4C). The first column to the right indicates the orientation of the fragment relative to the minimal promoter. F (forward) and R (reverse) indicate whether the 3' or 5' end was closest to the promoter. The second column shows the distribution of primary transformants that showed no (n), weak (w), intermediate (i), or strong (s) staining [see (B)]. The third column indicates whether and how strongly a representative line stained in an *AG*-typical pattern during stage 3 of flower development (n/d, not determined). Although



many KB11 and K13 lines showed *GUS* expression, the early pattern was not *AG*-typical, but was throughout early flowers and the shoot apex, and in the stem. The fourth column indicates relative activity in a *lfy-12* background. The fifth column indicates whether or not activity was increased in *LFY:VP16*. The last column indicates the number of lines analyzed for each construct. A restriction map is shown below. B, BamH I; Bc, Bcl I; H2, Hinc II; H3, Hind III; N, Nla IV; Sc, Sca I; Sn, SnaB I; Sp, Spe I; Ss, Ssp I; X, Xba I. (B) Examples of weak, intermediate, and strong *GUS* staining in whole apices of different reporter lines (from left to right, MX68 line 38; KB31 line VIIIC1; KB31 line VIIIC7). A mid-stage 3 flower (20) is indicated in each apex. Faint staining in the left apex is indicated by arrowheads.

The Salk Institute for Biological Studies, 10010 North Torrey Pines Road, La Jolla, CA 92037, USA.

\*These authors contributed equally to this work.

†To whom correspondence should be addressed. E-mail: weigel@salk.edu

## REPORTS

hancers that are both necessary and sufficient for the wild-type *AG* expression pattern, as demonstrated by placing this fragment upstream of a minimal heterologous promoter linked to GUS (reporter KB9; Figs. 1 and 2B). The KB9 reporter responded to changes in *LFY* activity in the same way as endogenous *AG*, indicating that it contains important *LFY*-responsive enhancer sequences. The onset of GUS expression was delayed in strong *lfy* mutants, whereas GUS was expressed earlier and ectopically in *LFY:VP16* plants (Fig. 2, A to C) (13). The 3-kb Hind III fragment is likely to confer most, if not all, of the *AG* response to *LFY*, because a GUS fusion containing the *AG* promoter, but not the large intron (11), does not respond to *LFY:VP16* (14).

From deletion analysis of the 3-kb Hind III fragment, we identified at least two redundant enhancers that could drive GUS expression in young wild-type flowers in a pattern that was similar to that of GUS under the control of the full-length 3-kb fragment (Figs. 1 and 2). For example, the nonoverlapping fragments present in KB14 (5' enhancer) and KB31 (3' enhancer) both conferred GUS expression in the center of young flowers, resembling the pattern of endogenous *AG* (Fig. 2, E and N). The response of the various reporters to changes in *LFY* activity revealed several additional features of *AG* regulation.

First, there appear to be synergistic enhancers that mediate the action of *LFY*-independent activators of *AG*, because GUS expression of the smaller reporters was generally more sensitive to loss of *LFY* activity than that of the full-length reporter (Fig. 2). Second, there appear to be cryptic regulatory elements that have overlapping roles in repressing *AG* in different regions of the flowers. For example, GUS was ectopically expressed in the outer whorls, but much less so in the floral stem or pedicel of *LFY:VP16* flowers carrying the KB18 reporter (Fig. 2L). In contrast, ectopic GUS expression was more consistent in the pedicel than in the first whorl of *LFY:VP16* flowers carrying KB14 (Fig. 2F).

We focused on the 3' enhancer because the smallest 3' fragment that was active on its own was considerably smaller than the minimal active element that we could define in the 5' portion of the full-length reporter (Fig. 1). In addition, GUS activity was much reduced in older flowers of plants carrying reporters containing only the 3' enhancer, which we thought would simplify the interpretation of expression patterns in mutant backgrounds.

As is not uncommon in enhancer analyses, simple deletions progressively reduced activity of the 3' enhancer. Nevertheless, we could track *LFY* responsiveness using *LFY:VP16*, which apparently bypasses the require-

ment for other positive factors. Several reporters that were either inactive or only weakly active in a wild-type background were reactivated when introduced into *LFY:VP16* (Fig. 3, A and B). We could thus map a *LFY*-response element to the overlap of *AG* sequences in KB24 and KB28, which share a common region of 230 base pairs (bp) (Fig. 1). Because *LFY* can bind to DNA (10), we investigated whether *LFY* could bind to the 3' *AG* enhancer. Using immunoprecipitation of DNA-protein complexes (15) followed by electromobility shift assays with overlapping subfragments spanning the 3' enhancer, we found that *LFY* bound to two sites (*AG* I and *AG* II) that are only 31 bp apart and that are located in the *LFY*-response element defined with the *LFY:VP16* experiments (Fig. 4). The sequences of the two *AG* sites are similar to each other as well as to the previously defined *LFY* binding site in the promoter of the *API* gene (10). *LFY* bound both *AG* sites with similar affinity, but did not bind either *AG* site as strongly as it did the *API* site (15).

We tested the in vivo relevance of the *LFY* binding sites defined in vitro by introducing two small deletions into the 3' *AG* enhancer. When the *AG* I site was deleted in

**Fig. 2. (A to O)** GUS expression in *AG* reporter lines KB9, KB14, KB21, KB18, and KB31. Apices were stained for GUS activity with X-gluc (5-bromo-4-chloro-indolyl- $\beta$ -D-glucuronic acid), embedded, sectioned, and viewed under dark-field illumination. Weak staining appears orange, and strong staining pink to purple. Asterisks indicate shoot apical meristems, numbers indicate stages of flower development (20). Note failure of GUS expression to expand completely into the first whorl (arrow-head) of KB14 *LFY:VP16* in (F), and failure of GUS expression to expand completely into pedicels (p) of KB18 *LFY:VP16* in (L). In contrast, GUS expression is obvious throughout the first whorl and pedicel in KB9 *LFY:VP16* in (C) and KB31 *LFY:VP16* in (O). All panels are at the same magnification ( $\times 58$ ).

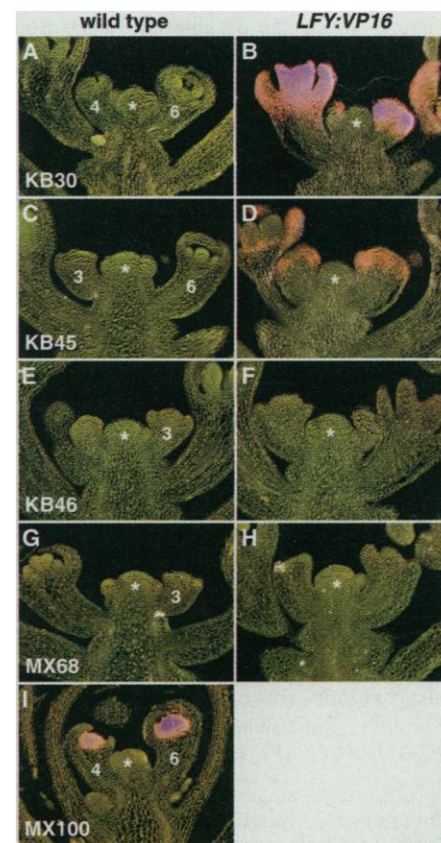
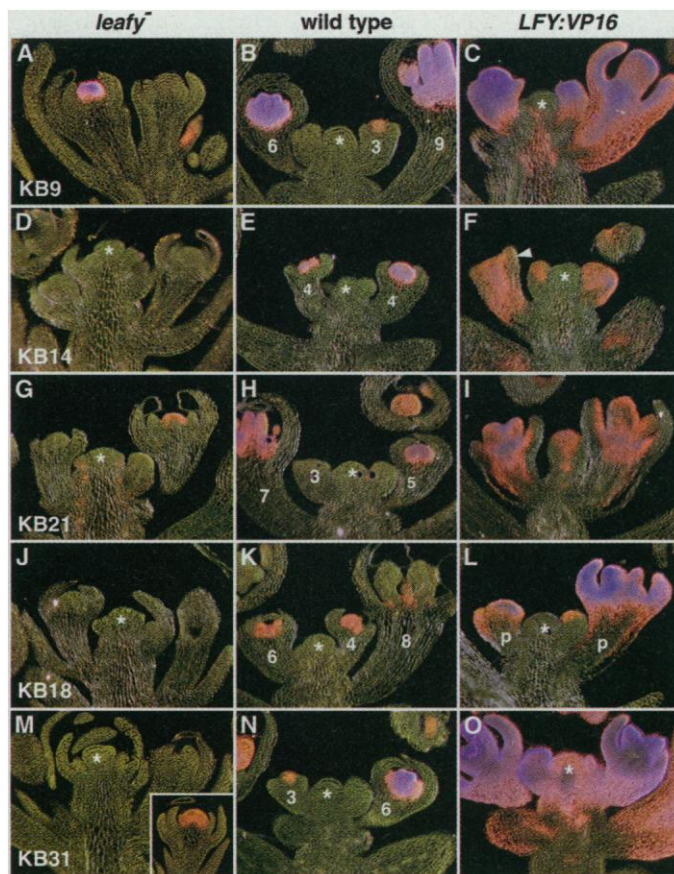


**Fig. 3. (A to I)** GUS expression in *AG* reporter lines KB30, KB45, KB46, MX68, and MX100. Specimens were prepared as in Fig. 2.

REPORTS

reporter KB45 (16), the GUS expression pattern was still in an *AG*-typical manner, but the expression levels were weak and only detectable in whole mounts, not in sectioned tissue (Fig. 3C). KB45 expression increased in response to *LFY:VP16* (Fig. 3D), although the response was attenuated compared with other reporters without an internal deletion (compare, for example, to Fig. 3, A and B). This result suggests that both LFY binding sites are required for in vivo activity of the 3' *AG* enhancer, and that the LFY binding sites are only partially redundant. One possible explanation is cooperative action of adjacent LFY binding sites in vivo, even though there is no evidence for cooperative in vitro binding of LFY to *AG* I and *AG* II sites (Fig. 4A).

The activity of the KB46 reporter, in which both the *AG* I and *AG* II sites were deleted (16), was even further reduced than that of the *AG* I deletion, KB45 (Fig. 3E). And in contrast to KB45, KB46 expression could not be restored by crossing it to *LFY:VP16* (Fig. 3F). To corroborate that the loss of enhancer activity was indeed due to loss of LFY binding sites, we tested the effects of a series of point mutations in the LFY binding sites. A 2-bp mutation eliminates binding of LFY to a site in the *API* promoter (10). The equivalent 2-bp mutations

(m1) eliminated in vitro binding of LFY to either *AG* site (Fig. 4, B and C). Single-base pair mutations (m2) in the center of the consensus LFY binding sites (Fig. 4C), although only 2 bp away from the m1 mutations, did not affect LFY binding (Fig. 4, B and C). The mutant *AG* I and *AG* II sites were introduced into the 3' *AG* enhancer, yielding reporters MX68 (*AG* I m1 and *AG* II m1) and MX100 (*AG* I m2 and *AG* II m2). The m1 mutations, which abolished in vitro binding of LFY, largely eliminated in vivo activity of the 3' enhancer (Figs. 1B and 3G). In contrast, the m2 mutations did not interfere with in vitro binding of LFY and did not affect in vivo activity of the 3' *AG* enhancer (Fig. 3I). To confirm that the LFY binding sites identified in vitro were indeed responsible for LFY action in vivo, we crossed several MX68 lines to *LFY:VP16*. In contrast to the control reporter KB31, or even reporters such as KB24 and KB28 that had the wild-type LFY binding sites but were otherwise too small to be active in a wild-type background, MX68 expression did not increase in *LFY:VP16* (Fig. 3H).

In contrast with many other transcription factor genes, *LFY* is not part of a gene family. *LFY* homologs have been cloned from several species of dicotyledonous plants (17), and each species seems to contain only one functional *LFY* homolog per haploid genome. Thus, we have little concern that related family members with similar DNA binding specificities as LFY bind in vivo to the LFY binding sites identified in vitro. Furthermore, there was a close correlation between the ability of LFY to bind to mutated sites in vitro and the in vivo activity of the corresponding reporters. Finally, we have been able to validate our results by probing DNA-protein interactions in vivo with the activated form of LFY, LFY:VP16. Together, these results support the hypothesis that binding of LFY is critical for transcriptional activation mediated by the 3' *AG* enhancer. Although this finding does not necessarily imply that LFY interacts directly with the basal transcription machinery to stimulate *AG* RNA expression, it makes LFY formally an *AG* activator.

Having recognized LFY as a direct activator of *AG* opens the way to identifying the coregulators that determine why *AG* is normally activated only in a subset of LFY-expressing cells. Previous studies have emphasized negative control of *AG* by *API*, *APETALA2*, *LEUNIG*, and *CURLY LEAF*, as well as the presumed *Arabidopsis* orthologs of the snapdragon genes *FISTULATA* and *STYLOSA* (6, 9, 18). None of our reporters was ectopically expressed in wild-type flowers in a pattern that resembled *AG* expression in plants mutant for negative regulators, suggesting that activation and repression of *AG* are intimately linked. To discover how region-specific expression of

*AG* is achieved, the sequences through which *AG* regulators other than *LFY* act need to be delineated.

References and Notes

1. M. Yanofsky, *Annu. Rev. Plant Physiol. Plant Mol. Biol.* **46**, 167 (1995); D. Weigel and O. Nilsson, *Nature* **377**, 495 (1995); M. A. Mandel and M. F. Yanofsky, *ibid.*, p. 522.
2. E. A. Schultz and G. W. Haughn, *Plant Cell* **3**, 771 (1991); D. Weigel, J. Alvarez, D. R. Smyth, M. F. Yanofsky, E. M. Meyerowitz, *Cell* **69**, 843 (1992).
3. E. Huala and I. M. Sussex, *Plant Cell* **4**, 901 (1992).
4. H. Ma, *Genes Dev.* **8**, 745 (1994); D. Weigel and E. M. Meyerowitz, *Cell* **78**, 203 (1994); J. L. Riechmann and E. M. Meyerowitz, *Biol. Chem.* **378**, 1079 (1997).
5. J. L. Bowman, D. R. Smyth, E. M. Meyerowitz, *Plant Cell* **1**, 37 (1989); M. F. Yanofsky *et al.*, *Nature* **346**, 35 (1990); J. L. Bowman, D. R. Smyth, E. M. Meyerowitz, *Development* **112**, 1 (1991); Y. Mizukami and H. Ma, *Cell* **71**, 119 (1992).
6. G. N. Drews, J. L. Bowman, E. M. Meyerowitz, *Cell* **65**, 991 (1991).
7. D. Weigel and E. M. Meyerowitz, *Science* **261**, 1723 (1993).
8. S. S. Hantke, R. Carpenter, E. S. Coen, *Development* **121**, 27 (1995).
9. P. C. McSteen, C. A. Vincent, S. Doyle, R. Carpenter, E. S. Coen, *ibid.* **125**, 2359 (1998).
10. F. Parcy, O. Nilsson, M. A. Busch, I. Lee, D. Weigel, *Nature* **395**, 561 (1998).
11. L. E. Sieburth and E. M. Meyerowitz, *Plant Cell* **9**, 355 (1997).
12. *AG* genomic sequences (nucleotides 44,331 to 47,358 of BAC F13C5, GenBank AL021711) were from pCIT526 (17). The fragment used in Fig. 4B spans nucleotides 46,832 to 46,992.
13. Lines used were *lfy-12* (3) and *LFY:VP16* DW245.2.7 (10).
14. F. Parcy and D. Weigel, unpublished data.
15. M. A. Busch and D. Weigel, unpublished data.
16. KB45 deletes nucleotides 46,873 to 46,901; KB46 deletes 46,873 to 46,949 (12).
17. E. S. Coen *et al.*, *Cell* **63**, 1311 (1990); A. J. Kelly, M. B. Bonlander, D. R. Meeks-Wagner, *Plant Cell* **7**, 225 (1995); J. Hofer *et al.*, *Curr. Biol.* **7**, 581 (1997); E. Souer *et al.*, *Development* **125**, 733 (1998); S. G. Southerton *et al.*, *Plant Mol. Biol.* **37**, 897 (1998).
18. K. D. Jofuku, B. G. W. den Boer, M. Van Montagu, J. K. Okamoto, *Plant Cell* **6**, 1211 (1994); Z. Liu and E. M. Meyerowitz, *Development* **121**, 975 (1995); J. Goodrich *et al.*, *Nature* **386**, 44 (1997); P. Motte, H. Saedler, Z. Schwarz-Sommer, *Development* **125**, 71 (1998).
19. GUS fusions were in pDW294, a pCGN1547 derivative [K. E. McBride, K. R. Summerfelt, *Plant Mol. Biol.* **14**, 269 (1990)] with the minimal -46-bp cauliflower mosaic virus promoter [P. N. Benfey and N.-H. Chua, *Science* **250**, 959 (1990)] upstream of *GUS* [R. A. Jefferson, T. A. Kavanagh, M. W. Bevan, *EMBO J.* **6**, 3901 (1987)]. Transgenic plants in the Columbia ecotype were generated by vacuum infiltration [N. Bechtold, J. Ellis, G. Pelletier, *C.R. Acad. Sci.* **316**, 1194 (1993)]. GUS staining was as described [M. A. Blázquez, L. Soowal, I. Lee, D. Weigel, *Development* **124**, 3835 (1997)].
20. D. R. Smyth, J. L. Bowman, E. M. Meyerowitz, *Plant Cell* **2**, 755 (1990).
21. Electromobility shift assays were performed with purified His-tagged LFY protein (10).
22. We are grateful to T. Nguyen for technical assistance. We thank M. Blázquez, M. Deyholos, R. Hong, K. Jones, O. Nilsson, F. Parcy, L. Sieburth, D. Wagner, and M. Yanofsky for discussion, review of the manuscript, and communicating unpublished results. Supported by a fellowship from the Human Frontier Science Program Organization (M.B.), and grants from the NSF and Department of Energy (D.W.). D.W. is a NSF Young Investigator.

12 March 1999; accepted 3 June 1999

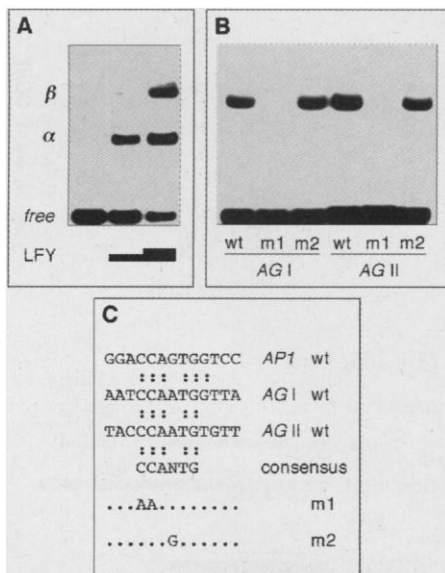


**Fig. 4.** Mapping of LFY binding sites in *AG*. (A) In vitro binding of LFY to a 160-bp fragment (12) from the *AG* 3' enhancer (21). At low protein concentration, one DNA-protein complex ( $\alpha$ ) is seen, whereas at higher protein concentration, a second, more slowly migrating complex ( $\beta$ ) appears. We interpret the  $\alpha$  complex as representing one site and the  $\beta$  complex as representing two sites occupied by LFY. (B) Binding to double-stranded, 30-bp oligonucleotides spanning the *AG* I and *AG* II sites (wt, wild type). (C) Comparison of LFY binding sites in *AG* with the previously reported site in *API* (10). The central bases form an inverted repeat in all three sites ("consensus").